# A fractal fracture model and application to concrete with different aggregate sizes and loading rates

Kug Kwan Chang[†]

*Architectural Engineering Department, Seoul National University of Technology, Seoul 139-743, South Korea*

Yunping Xi[‡]

*Department of Civil, Environmental and Architectural Engineering, University of Colorado, Boulder, CO 80309, USA*

Y-S Roh[‡†]

*Architectural Engineering Department, Seoul National University of Technology, Seoul 139-743, South Korea*

**Abstract.** Recent developments in fractal theory suggest that fractal may provide a more realistic representation of characteristics of cementitious materials. In this paper, the roughness of fracture surfaces in cementitious material has been characterized by fractal theory. A systematic experimental investigation was carried out to examine the dependency of fracture parameters on the aggregate sizes as well as the loading rates. Three maximum aggregate sizes (4.76 mm, 12.7 mm, and 19.1 mm) and two loading rates (slow and fast loading rate) were used. A total of 25 compression tests and 25 tension tests were performed. All fracture parameters exhibited an increase, to varying degrees, when aggregates were added to the mortar matrix. The fracture surfaces of the specimens were digitized and analyzed. Results of the fractal analysis suggested that concrete fracture surfaces exhibit fractal characteristics, and the fractal geometry provide a useful tool for characterizing nonlinear fracture behavior of concrete. Fractal dimension D was monotonically increased as maximum aggregate sizes increase. A new fractal fracture model was developed which considers the size and shape of aggregate, and the crack paths in the constituent phases. Detailed analyses were given for four different types of fracture paths. The fractal fracture model can estimate fractal dimension for multiphase composites.

**Keywords:** fracture; fractal; roughness; aggregate size; loading rate.

## 1. Introduction

Fracture properties of concrete cannot be fully characterized by conventional linear elastic fracture mechanics. Therefore, quantitative description of fracture surface and correlation between the

---

† Associate Professor
‡ Professor
‡† Full-time Lecturer, Corresponding author, E-mail: rohys@snut.ac.kr

features of internal structure and fracture surface of concrete has been a research topic of great interest in recent years (Carpinteri *et al.* 2004, Issa *et al.* 2003, Li *et al.* 1995, Xie 1993). Observations on fracture surfaces of concrete indicated that different fracture processes could be characterized by different fracture surface topographies. Hence, quantitative characterization of fractography becomes very important for understanding fracture properties of concrete. It provides us with valuable information about energy absorption in the process of fracture, and it bridges the gap between micro-mechanical behaviors of the fracture and the corresponding macroscopic fracture behavior of quasibrittle solids, such as concrete.

Using different size of wedge-splitting specimen, Issa *et al.* (2003) found that there is an increase in fracture toughness with increasing specimen size and maximum aggregate size. For the same concrete mix, they observed that when a crack tip meets an aggregate particle, it propagates along the matrix-aggregate interface, and then re-enters the matrix. Larger aggregate particles result in a greater area of crack surface than smaller particles and thus, more energy is required for the crack to propagate. Similar observations can be found in other literatures (Li *et al.* 1995, Perdikaris and Romeo 1995, Roh and Xi 2001). For instance, Perdikaris and Romeo (1995) reported that for both normal and high strength concrete with 25 mm (1 in.) aggregate, the fracture energy of concretes is about twice the fracture energy containing 6 mm (0.25 in.) aggregate. This is because for concrete with larger aggregate, there is a higher degree of matrix-aggregate interlock, resulting in an increase in energy required for crack propagation.

On the other hand, for concrete specimens with the same aggregate sizes, the characteristics of fracture surface vary with the loading rates (Zhang *et al.* 2001). In general, for the same material, different loading rates result in completely different fracture surfaces. For concrete in particular, slow loading rates cause rougher fracture surfaces, and rapid loading rates result in smoother surfaces. This is due to the fact that cracks tend to go around aggregates under a slow loading rate, and penetrate through aggregates under a fast loading rate. So, the features of fracture surface of concrete depend on loading rate as well as aggregate size.

In the present study, the effects of both aggregate size and loading rate on the fracture properties of concrete are studied experimentally. The characteristics of fracture surface of concrete are evaluated by fractal theory. The experimental study was briefly described in a short paper (Roh and Xi 2001). The main purpose of this paper is to establish a quantitative correlation among the fractality (fractal dimension, or roughness) of fracture surface of concrete, the degree of heterogeneity (size of the aggregate), and the loading rate. A carefully designed experimental program was conducted and a theoretical model was developed based on the obtained test data.

## 2. Experimental program

The main testing variables were the maximum aggregate sizes, $d_{max}$, and loading rates. Aggregate grading is listed in Table 1. Four different aggregate sizes were used in the study. With different sizes of aggregates, specimens were called hardened cement paste without any aggregate, mortar with fine sand, concrete with fine aggregate, and concrete with coarse aggregate. Two different loading rates were used: static loading rate ($2.5 \times 10^{-2}$ to $2.5 \times 10^{-3}$ mm/sec.) and moderately fast loading rate (1.5 to 2.5 mm/sec.). The size of concrete specimen is fixed: 10 cm by 20 cm concrete cylinders. The water-cement ratio was kept as a constant $w/c = 0.5$, except for the cement paste specimens, in which $w/c = 0.45$ was used. The other concrete mix parameters, such as sand to

Table 1 Aggregate grading

| Sieve size | % of passing by *wt* | ASTM C33 Limits |
|:---:|:---:|:---:|
| 0.5 mm | 100 | 100 |
| No. 4 | 94 | 95 to 100 |
| No. 8 | 81 | 80 to 100 |
| No. 16 | 68 | 50 to 85 |
| No. 30 | 37 | 25 to 60 |
| No. 50 | 12 | 10 to 30 |
| No. 100 | 0 | 2 to 10 |

gravel ratio and gradation of aggregate were kept the same in order to eliminate the possible influences.

Two different loading configurations were used: direct compression test and splitting tension test. It should be noted that fracture surface due to tensile failure can also be characterized by the three point bending test. The splitting tension test was selected in the present study simply for convenience: the same set of compressive platen on the loading machine can be used for both the tension and the compression test. 25 specimens in compression and 25 specimens in splitting tension were tested.

## 3. Fractal surface profiles

Previous researches showed that the fracture surface of composite materials could be effectively described by fractal geometry (Lung and Mu 1987, Lange *et al.* 1993). There are numerous devices and methods for tracing and recording the profile of a fracture surface. A three-dimensional scanner was used in the present study for evaluating fracture surface profiles. A mechanical probe is in contact with fracture surface, and elevations (the distance from the starting probe position to crack surface) are measured at a regular interval along the crack profile with 15 $\mu m$ resolution. The maximum scanning length is 0.1 m. The topological information provided by the 3D scanner is then used to determine surface roughness number (RN), which is defined as $RN(\delta) = A_a(\delta)/A_o(\delta)$, where $\delta$ is the grid size or measurement interval; $A_a$ and $A_o$ are the actual surface area and the projected surface area between the grids, respectively. The sum of all elemental areas provides an approximation for the area of actual surface. Thus, the roughness number of a fracture surface can be calculated as $RN = \Sigma\Delta A_a(\delta)/\Sigma\Delta A_o$.

From the experimentally determined RN, the fractal dimension of a surface, D, can be evaluated, which is defined as $A_a(\delta) = A_o r^{-(D-d)}$, where $d$ is the topological dimension ($d = 1.0$ for the line profile estimation and $d = 2.0$ for area profile estimation), and $r$ is a unit length scale. The fractal dimension, *D*, can be evaluated by plotting the roughness number versus the measurement size in a Richardson plot (1961). The slope of the linear region in the log-log plot can be given by the relationship $D = d - slope$.

Figs. 1 to 4 show the fracture surfaces obtained by the 3-dimensional scanner from direct compression specimens with different aggregate sizes at the static loading rate. The lower and upper bound of measurement scale was from 15 $\mu m$ to 0.1 *m*. The measurement scale is a very important issue because it was found recently that fractal dimension depends on the scale. Various fractal

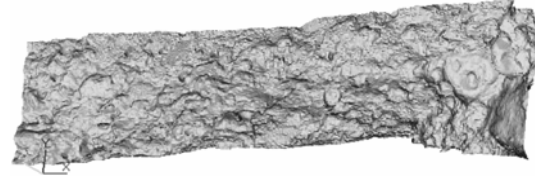Fig. 1 Surface profile of cement paste

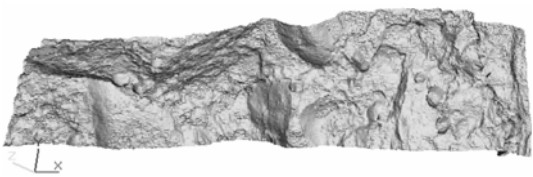

Fig. 2 Surface profile of mortar



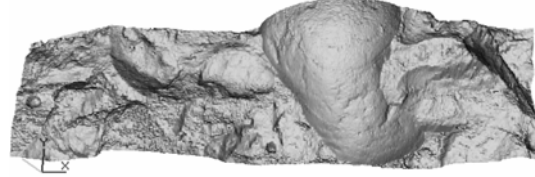Fig. 3 Surface profile of concrete with fine aggregate



Fig. 4 Surface profile of concrete with coarse aggregate

measurement scales were proposed by other researchers recently (Dougan and Addison 2001, Saouma and Barton 1994, Wang and Diamond 2001). Dugan and Addison (2001) suggested a lower bound of measurement scale as 0.63 to 4.57 nm corresponding to the range of C-S-H structure. However, considering the same C-S-H scale, Saouma and Barton (1994) estimated the scale to be approximately 10 $\mu m$. Wang and Diamond (2001) observed different regimes of fractal dimension from 1 $\mu m$ to 2.5 $\mu m$ scale. Due to the absence of lower bound of measurement scale, two major confusions were caused. One is to define fracture energy considering fractal fracture surfaces. In this case, fracture surface will have infinite area as measurement scale gets smaller, and so the propagation of fractal cracks becomes impossible. The other is that there is no unified agreement on fractal dimension of fractured surfaces for various materials. For instance, fractal dimension of ice fragmentation varies from 2.15 to 2.61 which are very high comparing the fractal dimension of fracture surface of concrete. Fractal dimension of steel has been measured as 2.179 to 2.266 by Trefilov *et al.* (2001), in case of rocks, the fractal dimension ranges between 1.027 and 1.068, reported by Zhang *et al.* (2001). Fractal dimensions of concrete fracture surfaces by many other researchers showed a large variation as depicted in Table 2.

The upper bound of measurement scale is also needed to measure fractal dimension of fractured surface of concrete due to the presence of large aggregates. Using fractal measurement scale which is less than the size of maximum aggregates may describe only the fractal dimension of aggregate

Table 2 Fractal dimension of concrete fracture surfaces

| Researchers | Fractal dimension |
|---|---|
| Lange *et al.* (1993) | around 2.1 |
| Issa *et al.* (2003) | 2.21~2.59 |
| Saouma and Barton (1994) | 2.06~2.12 |
| Chiaia *et al.* (1998) | 2.03~2.25 |
| Dugan and Addison (2001) | 2.0~2.4 |
| Roh and Xi (2001) | 2.05~2.2 |

surface, which apparently does not represent fractal dimension of whole fracture surface. Therefore, the measurement scale that is larger than the maximum aggregate size should be included as an upper bound of measurement scale. The maximum measurment scale $r_{max}$ can be proposed based on this study as $r_{max} = 1.5 \cdot d_{max}$ where $d_{max}$ is the maximum aggregate size. And minimum measurement scale can be suggested as 10 $\mu m$ to 20 $\mu m$, which can fully represent smallest aggregate sizes.

## 4. The experimental results

Figs. 5 and 6 show maximum aggregate size versus compressive strength and splitting tension strength of concretes. One can see that both tensile and compressive strength increases with
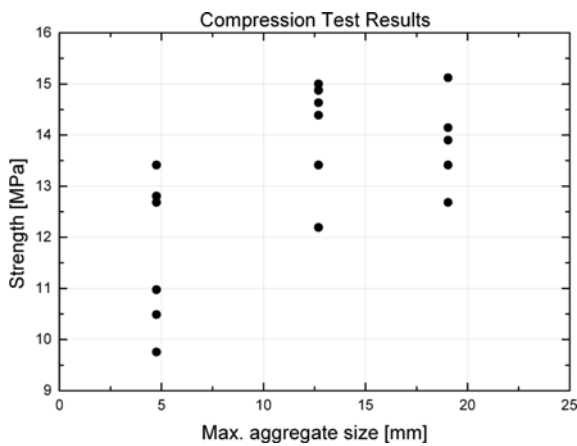


Fig. 5 Strength vs. Max. aggregate sizes for compression test
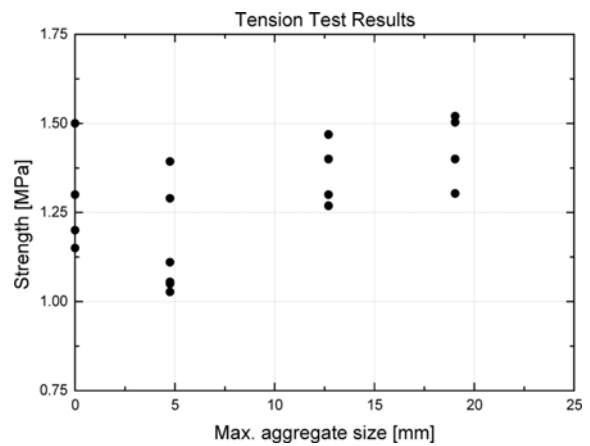
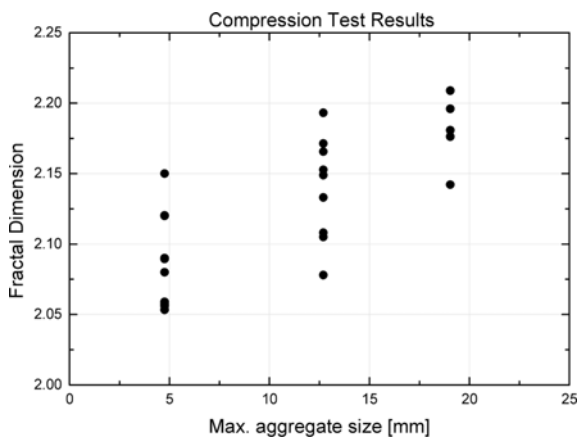Fig. 6 Strength vs. Max. aggregate sizes for tension test



Fig. 7 Fractal dimension vs. Max agg. sizes for compression test
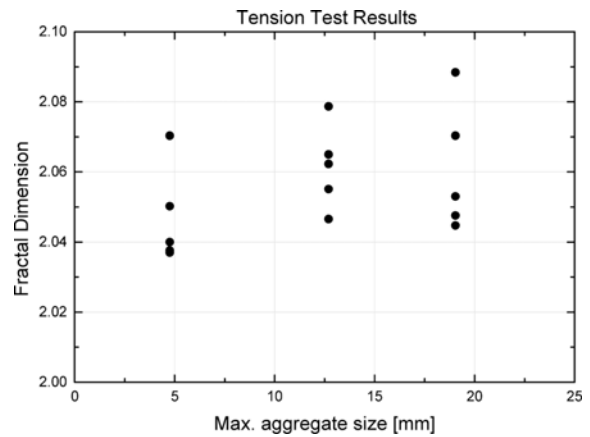
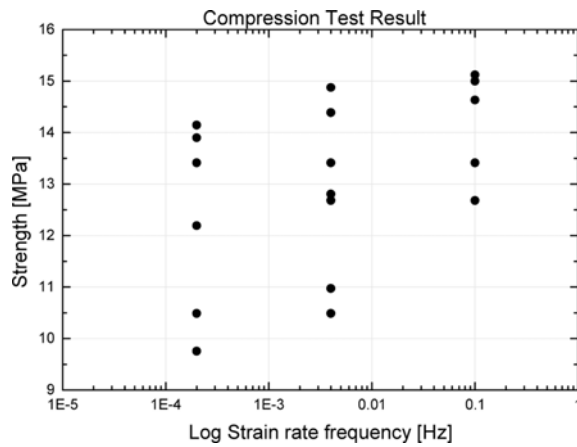Fig. 8 Fractal dimension vs. Max agg. sizes for tension test

Fig. 9 Strength vs. Loading rates for compression
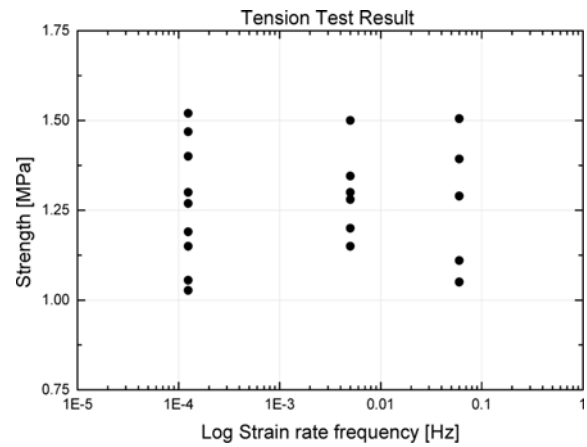


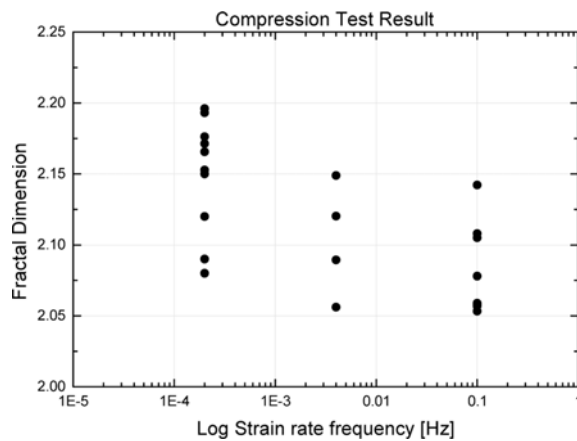Fig. 10 Strength vs. Loading rates for tension



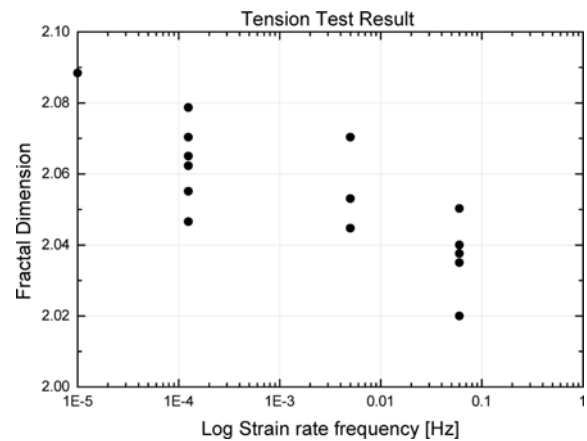Fig. 11 Fractal dimension vs. Loading rates



Fig. 12 Fractal dimension vs. Loading rates

increasing aggregate sizes (Fig. 5). The tensile strength increased about 15%, and the compressive strength increased even more. As shown in Figs. 7 and 8, the fractal dimension also increases with increasing aggregate size for both compression and tension specimen. In Figs. 5 to 8, the increases in strength and fractal dimension are larger in case of compressive loading than tensile loading (splitting tension) case. It was also found that fracture surface of cement paste exhibited a fractal dimension of 2.03, similar to the value reported in Wang and Diamond (2001) for the same measurement scale. However, fractal dimension of mortar surface was found around 2.16 at Wang and Diamond (2001), and this value is higher than that of present test results (2.05~2.12) in Fig. 6. The present experimental results are consistent with other test results (Issa *et al.* 2003, Lange *et al.* 1993, Saouma and Barton 1994, Wang and Diamond 2001, Bentur and Mindess 1986).

Figs. 9 and 10 show the effect of loading rate on strength of concrete. One can see that compressive strength is increased at higher loading rate (Fig. 9). In the case of tensile loading, tensile strength was not enhanced due to fast loading (Fig. 10). This probably is due to the limited range of loading rate used in this study. The upper limit of MTS machine available was not high

enough to induce strength enhancement due to fast loading rate.

Bentur and Mindess (1986) compared crack patterns in different types of plain concrete subjected to bending with different loading rates. They observed that cracks in normal strength concrete tend to form around the aggregate particles, passing along the matrix-aggregate interface. At a higher loading rate (250 mm/min.), cracks propagate through the aggregate particles, resulting in straight crack path. Their study for the crack propagation was carried out with contoured double cantilever beams. From experimental results obtained in the present study, similar observations were obtained. The fracture surface is smoother under higher loading rate, while the surface is rougher under slower loading rate. The difference of surface roughness due to loading rate can be characterized quantitatively by fractal dimension. Although there are large scattering in experimental data, one can still see the basic tendency from Figs. 11 and 12: the average fractal dimensions for compression and tension decrease with increasing loading rate. Fractal dimensions obtained by two-dimensional analysis in this study were between 2.05 to 2.21 for compression and 2.03 to 2.08 for tension. This means that the fractal dimension is higher for compression than tension.

## 5. Basic fractal models for different fracture types

From the above experimental observations, one can see clearly that the roughness of fracture surface of concrete depends on aggregate sizes, loading rates, and loading configurations (tension or compression). In this section, we will develop some mathematical fractal model that take into account these influential parameters. Our intension is that for given aggregate size and loading configuration (at a fixed loading rate), for example, the fractal dimension of the fracture surface can be calculated by the mathematical models.

There are many possible scenarios of crack development in cementitious materials. Among these scenarios, four fracture types were selected in this study to simulate different fracture paths. The four fracture types were modeled based on fractal theory developed for rock mechanics by Xie (1993). Fractal dimensions of the four fracture types will be derived in this section. Three of the four fractal fracture types simulate a crack path going around an aggregate particle, and the other fractal fracture type simulates a crack path going through an aggregate. The major advantage of fractal fracture models is that the fractal dimension of a fracture surface can be correlated with volume fraction and size distribution of aggregates used in concrete. Various shape of aggregate can also be simulated using proposed model. The hexagon shape is selected as an example in this paper to demonstrate the formulation of new model. Using similar approach, aggregate shape can be varied to any shape by using correction factors.

A unit element of size $L_o \times w_o$ can be used to represent one section of crack path. The same unit element can be duplicated along the direction of the crack path, say $y$ direction. In the out of plane direction (direction-$z$), it is assumed that the unit element extends along this direction so that the one-dimensional profile can be simply expanded to a two-dimensional surface. If, for example, the fractal dimension $D = 1.2$ in one direction, then the fractal dimension of a two-dimensional surface composed of the unit element becomes $D = 2.2$. It should be mentioned that, in these fractal fracture models, the difference of fractal characteristics between the direction of crack propagation and transverse direction has not been considered (Chiaia *et al.* 1998). The following is the formulation of four fractal fracture types.
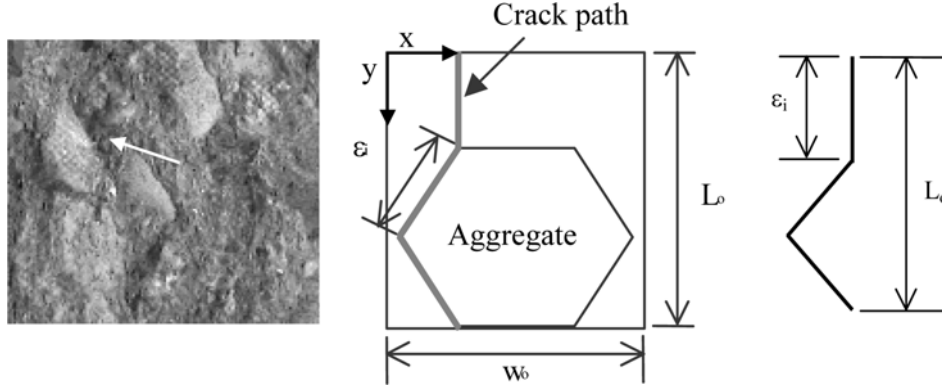
Fig. 13 The fractal fracture type A

## 5.1 Fractal fracture type A

The fractal fracture type A consists of matrix and aggregate with unit element $L_o \times \omega_o$. It is assumed that crack path starts from matrix part and propagates along the interface between matrix and aggregate as shown in Fig. 13. Only two sides of the hexagon-shaped aggregate are exposed to crack path (Fig. 13).

The photo shown in Fig. 13 (on the left) illustrates that two sides of aggregates are exposed to crack surface. Now, let us consider $N$ being the number of crack segments, $N = L_t / \varepsilon_i$ ($N = 3$ in this fractal fracture type), where, $L_t$ is the total length of crack path in fractal fracture type A. $\varepsilon_i$ is length of crack segment or length of one side of aggregate (called relative size of aggregate). The number of crack segments, $N$, is the summation of crack segments in matrix as well as in aggregate-matrix interface, $N = N_{matrix} + N_{agg}$. $r$ is defined as a ratio of similarity and it is a function of relative aggregate size $\varepsilon_i$. From the basic geometry and fractal theory, $r$ can be evaluated as:

$$r = \frac{\varepsilon_i}{L_o} = \frac{1}{1 + \sqrt{3}} \tag{1}$$

where $L_o$ is the height of unit element and has been chosen so that $\varepsilon_i$ is a constant for all three segments. $w_o$ is the width of one unit element. The fractal dimension is defined by:

$$D = \frac{\log N}{\log(1/r)} = 1.0931 \tag{2}$$

The volume fraction of aggregate can be calculated by:

$$V = \frac{V_{aggregate}}{V_{total}} = \frac{3\sqrt{3}}{2} \frac{\varepsilon_i^2}{w_o L_o} = 0.3481 \frac{L_o}{w_o} \tag{3}$$

## 5.2 Fractal fracture type B

Fractal fracture type B is the case that larger portion of aggregate surfaces is exposed in a crack path as shown in Fig. 14. Crack propagates along three sides of the hexagon (50% of aggregate exposure).
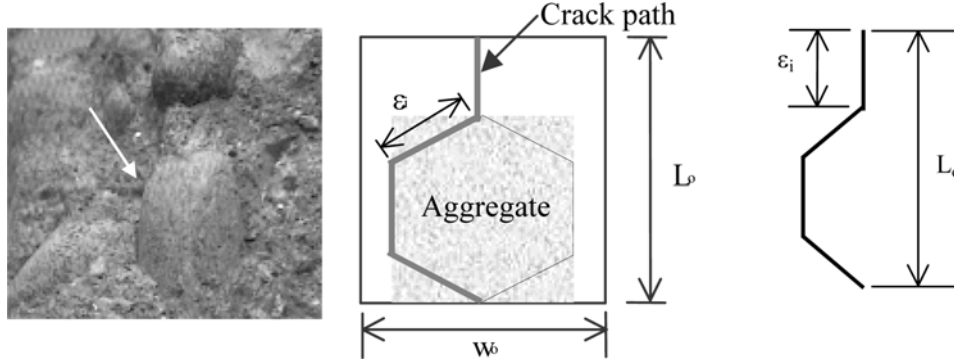
Fig. 14 The fractal fracture type B

A similar prcedure can be applied to derive fractal parameters for fractal fracture type B, which are $N = 4$, $r = 1/3$, $D = 1.262$, and $\overline{V}_{agg.} = 0.2887 L_o/w_o$. Comparing fractal dimensions of fractal fracture type A and type B, one can see that the larger the portion of aggregate exposed to crack, the higher the fractal dimension ($D = 1.0931$ for type A, $D = 1.262$ for type B). The fractal fracture type B contains less aggregate volume fraction compared to the fractal fracture type A, because $\varepsilon_{Ai}$ ($\varepsilon_i$ for the fracture type A) has a larger length at the fixed element $L_o$ and $w_o$.

## 5.3 Fractal fracture type C

Fractal fracture type C, as shown in Fig. 15, has 50% of aggregate exposure to crack path like fractal fracture type B, however, the aggregate is rotated 90° with respect to the longer aggregate axis.

This particular crack path has a dramatic change of crack angle (90°) when the crack deflects from matrix to aggregate. In this case, number of crack segments is 8. The other fractal parameters are $r = 1/(2 + 2\sqrt{3})$, $D = 1.2245$ and $\overline{V}_{agg.} = 0.3481 L_o/w_o$.
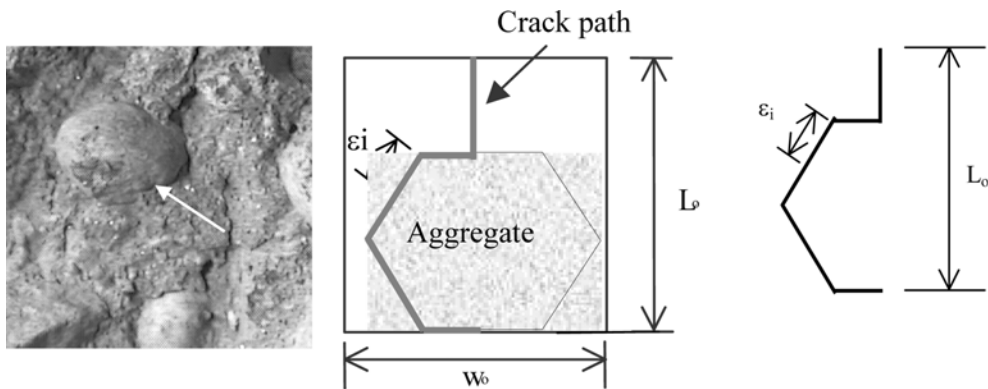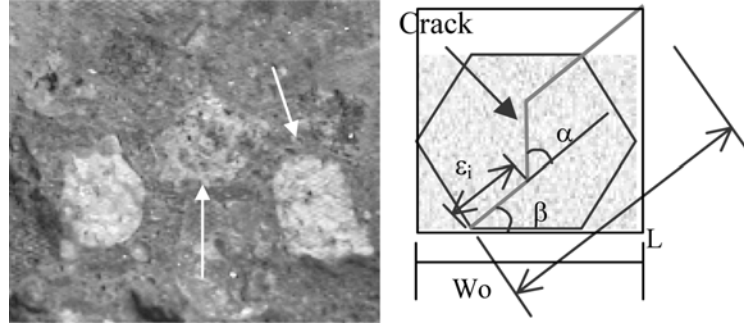


Fig. 15 The fractal fracture type C

Fig. 16 The fractal fracture type D

Table 3 Fractal parameters for fractal fracture type D

| $N = 4$ | $\alpha = 0°$ | $30°$ | $45°$ | $60°$ | $90°$ |
|---|---|---|---|---|---|
| $r = \dfrac{\varepsilon_i}{L_o} = \dfrac{1}{3 + \cos\alpha}$ | $\dfrac{1}{4}$ | $\dfrac{1}{3.866}$ | $\dfrac{1}{3.707}$ | $\dfrac{1}{3.5}$ | $\dfrac{1}{3}$ |
| $D = \dfrac{\log N}{\log(1/r)}$ | 1000 | 1.0252 | 1.0580 | 1.1066 | 1.2619 |
| $\overline{V} = \dfrac{V_{aggregate}}{V_{total}}$ | $0.3654\dfrac{L_o}{w_o}$ | $0.3678\dfrac{L_o}{w_o}$ | $0.3700\dfrac{L_o}{w_o}$ | $0.3712\dfrac{L_o}{w_o}$ | $0.3608\dfrac{L_o}{w_o}$ |

## 5.4 Fractal fracture type D

Due to fast loading rate or high strength of matrix and interface, cracks can propagate through the aggregate, resulting in a relatively smoother fracture surface, as shown in Fig. 16.

The fractal fracture type D is more complex than the other three types, because the crack orientation may change randomly, that is, crack may deflect by different angles inside aggregate. In order to simulate the change of crack orientation, deflection angle $\alpha$ is introduced (see Fig. 16). The deflection angle affects fractal dimension, which means that fractal parameters of this model depend on the deflection angle $\alpha$. From the geometry in Fig. 16, the relationship between $\alpha$ and $\beta$ can be easily found. Like all other fracture types, fractal fracture type D has the same length of crack segment $\varepsilon_i$. Table 3 shows fractal dimensions and volume fractions of fractal fracture type D with different angle $\alpha$. In the case that $\alpha$ is zero, crack has no deflection angle inside aggregate, going straightly through aggregate. Hence, the fractal dimension is simply 1.0, corresponding to a flat surface.

Now, for each maximum aggregate size used in strength tests, we can plot the corresponding fractal dimensions for four fractal fracture types. The results are shown in Figs. 17 to 20. In the figures, the fractal dimensions obtained from real fracture surfaces of compression and tension tests were also included as comparison. One can see that the fractal dimensions from four fractal models do not agree with the experimental data very well. This is because the solid and dashed lines in figures were calculated based on just one type of fractal fracture type and for one aggregate size.
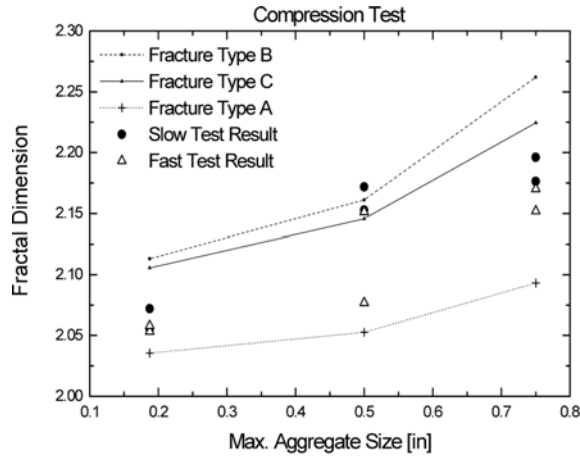
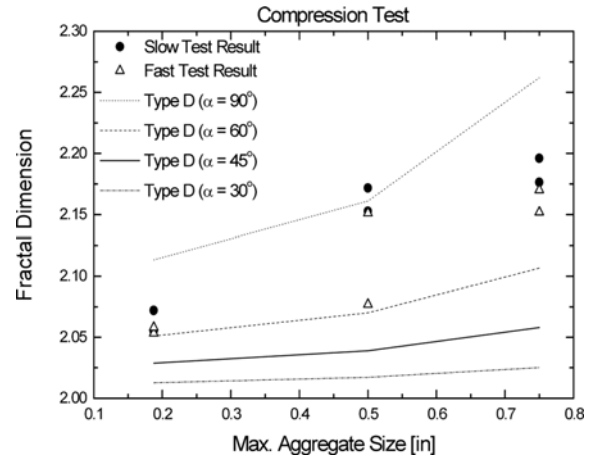Fig. 17 Fractal dimensions vs. Aggregate sizes for types A, B, and C



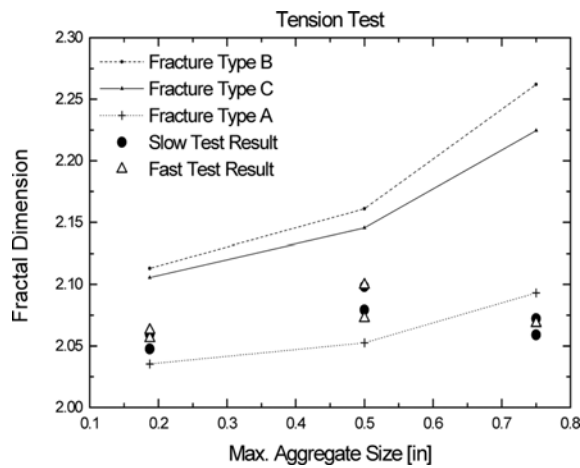Fig. 18 Fractal dimensions vs. Aggregate sizes for type D



Fig. 19 Fractal dimensions vs. Aggregate sizes for types A, B, and C
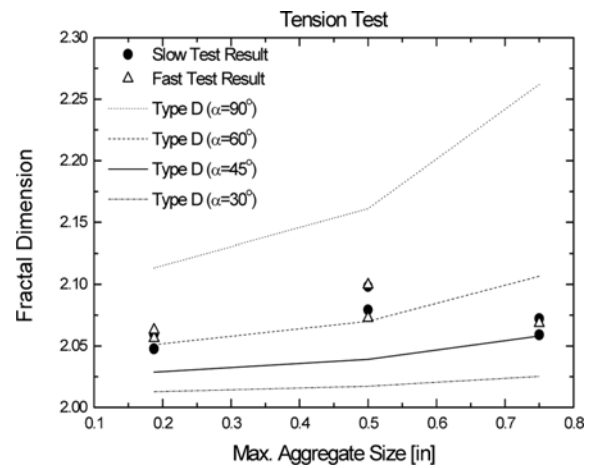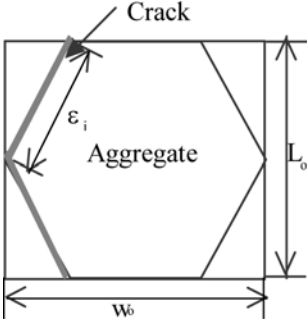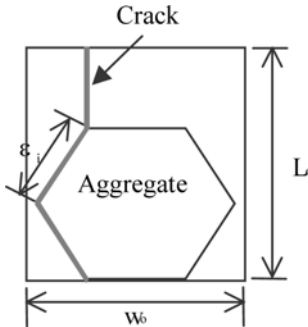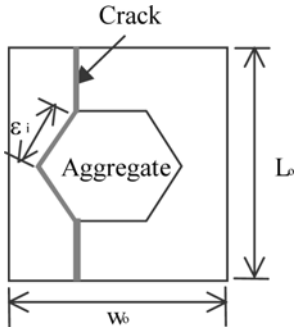


Fig. 20 Fractal dimensions vs. Aggregate sizes for type D

Visual observation on the experimental fracture surfaces showed that fracture surfaces of both compression and tension are not belong to any single type of fractal fracture type, but combinations of four different types. More specifically, the fracture surfaces of compression test look more like combinations of fractal fracture type B and type C rather than type A or type D. On the other hand, the fracture surfaces of tensile test look like combinations of fractal fracture type A and type D.

## 6. Fractal fracture model including different aggregate sizes

At this point, our models include only one size of aggregate and one type of fractal fracture. In a real fracture surface, many different aggregate sizes and fracture types are involved. In this section,

Table 4 Different aggregate sizes for fractal fracture type $A_i$

| $A_1$ | $A_2$ | $A_3$ |
|---|---|---|
|  |  |  |
| $N = 2$ | $N = 3$ | $N = 4$ |
| $\varepsilon_i = \dfrac{L_o}{\sqrt{3}}$ | $\varepsilon_i = \dfrac{L_o}{1 + \sqrt{3}}$ | $\varepsilon_i = \dfrac{L_o}{2 + \sqrt{3}}$ |
| $D = 1.2619$ | $D = 1.0931$ | $D = 1.0526$ |
| $d_{\max} = 1.1547 L_o$ | $d_{\max} = 0.7320 L_o$ | $d_{\max} = 0.5359 L_o$ |
| $V_i = 0.866 \dfrac{L_o}{w_o}$ | $V_i = 0.3481 \dfrac{L_o}{w_o}$ | $V_i = 0.1865 \dfrac{L_o}{w_o}$ |

fracture surfaces will be simulated by using different size of aggregate.

Different aggregate sizes can be simulated by fixing element unit size $L_o \times w_o$ for each fractal fracture type (Table 4). Since the number of crack segments is changing, fractal dimension also changes (different geometry). We introduce a subscript $i$ for each fractal fracture type, such as $A_i$. $A_2$ can be obtained from $A_1$ by adding one more segment to crack path in matrix, and this will make the relative size of aggregate smaller than $A_1$. In this manner, size of aggregate can be further reduced to $A_3$, $A_4$, ... etc. Different fractal dimension and volume fraction for each different sub-types are listed in Table 4.

The general expression of fractal parameter for each sub-types can be described by using $i$, $N = 2 + i$, where $i = 0, 1, ..., n$. General expression of the length of crack segment or size of aggregate, $\varepsilon_i$, can then be evaluated as,

$$\varepsilon_i = \frac{L_o}{i + \sqrt{3}} \tag{4}$$

Using the results of fractal fracture type A in Table 4, fracture surfaces from different aggregate size distributions can be simulated. Similarly, for fractal fracture types B, C, and D, the fractal parameters of the sub-types can be calculated in the same manners.

## 7. Compositions of fractal fracture model

As shown in Fig. 21, more than one type of fracture may appear in a real fracture surface.
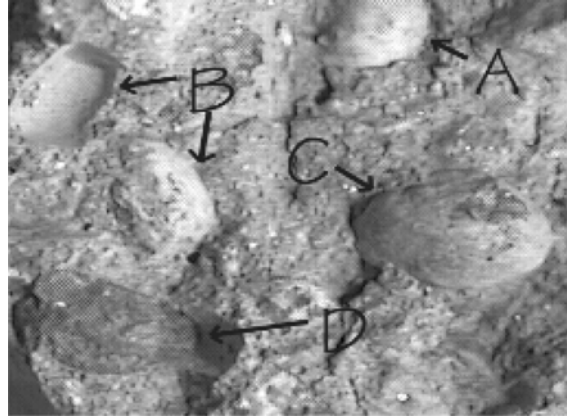
Fig. 21 Fracture surfaces showing all fractal fracture types



$$N = 7$$
$$L_o = (4 + \sqrt{3})\varepsilon_i$$
$$r = \frac{1}{(4 + \sqrt{3})}$$
$$D = \frac{\log 7}{\log(4 + \sqrt{3})} = 1.1144$$
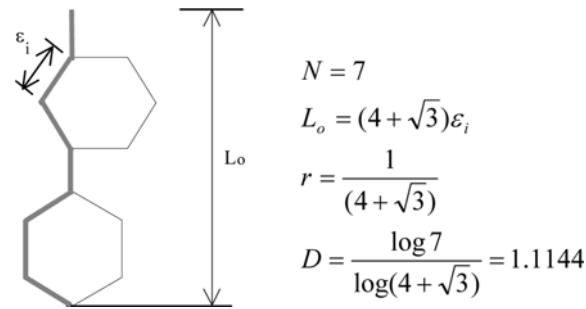
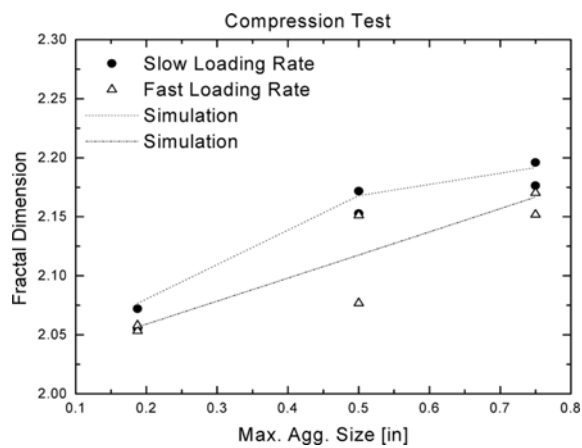Fig. 22 Combination of fracture types $A_2$ and $B_2$



Fig. 23 Simulation of fractal dimension for compressive loading test
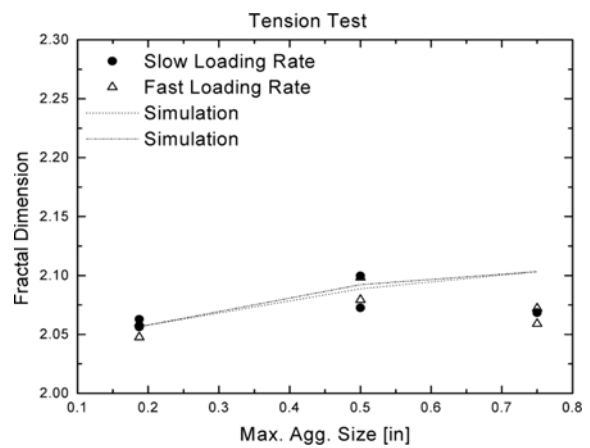


Fig. 24 Simulation of fractal dimension for tensile loading test

Therefore, it is important to consider various combinations of different fractal fracture types. Fig. 22 is an example of combination $A_2$ & $B_2$. Therefore, the fractal dimension of a particular fracture surface depends on fractal fracture types as well as aggregate sizes.

It is possible to combine all fracture types with various sizes of aggregates by using proposed fractal model. In this way, an actual fracture surface can be simulated by using a combination of fracture types and aggregate sizes. Figs. 23 and 24 show the comparisons of some simulations based on combined fractal dimensions with test results. As one can see, the results agreed with the test data very well, much better than the results shown in Figs. 17-20.

## 8. Conclusions

**Experimental study** - The fracture surface of concrete can be quantitatively characterized by the fractal theory. Fractal dimensions of concrete specimens with different aggregate sizes under different loading rates were measured. The difference of the fractal dimension under direct compression and splitting tension was experimentally studied and analyzed in detail.

1. The strength of concrete and fractal dimension of fracture surface of concrete increased with increasing aggregate sizes.
2. The compressive strength of concrete increases with loading rate. The strength enhancement due to high loading rate did not appear in the tension test, within the range of loading rates used in this study.
3. The fractal dimension decreased with increasing loading rate.

**Theoretical modeling** - A novel fractal fracture model is proposed, which is based on four basic fractal fracture types. In the new model, fractal parameters can be correlated to intrinsic parameters of the microstructure, such as sizes and volume fraction of aggregates. Various fracture paths in multi-phase composites can be considered and quantitatively evaluated. The size and shape of aggregate can also be incorporated in the fractal model. As numerical examples, fractal parameters of four different types of fracture paths were calculated. Fracture surfaces for concretes with different types of aggregates can be simulated by using the proposed fractal fracture model.

## Acknowledgements

## References

Bentur, A. and Mindess, S. (1986), "The effect of concrete strength on crack patterns", *Cement and Concrete Research*, **16**(1), 59-66.
Carpinteri, A., Chiaia, B. and Cornetti, P. (2004), "A mesoscopic theory of damage and fracture in heterogeneous materials", *Theoretical and Applied Fracture Mechanics*, **41**, 30-50.
Chiaia, B., van Mier, J.G.M. and Vervuit, A. (1998), "Crack growth mechanism in four different concretes: Microscopic observation and fractal analysis", *Cement and Concrete Research*, **28**, 103-114.

Dougan, L.T. and Addison, P.S. (2001), "Estimating the cut-off in the fractal scaling of fractured concrete", *Cement and Oncrete Research*, **31**, 1043-1048.

Issa, Mohesen A., Issa, Mahmoud A., Islam, M.S. and Chudnovsky, A. (2003), "Fractal dimension – A measure of fracture roughness and toughness of concrete", *Eng. Fracture Mech.*, **70**, 125-137.

Lange, D.A., Jennings, H.M. and Shah, S.P. (1993), "Relationship between fracture surface roughness and fracture behavior of cement paste and mortar", *J. American Ceramic Society*, **76**(3), 589-597.

Li, X.W., Tian, J., Kang, Y. and Wang, Z.G. (1995), "Quantitative analysis of fracture surface by roughness and fractal method", *Scripta Metallurgica et Materialia*, **33**(5), 803-809.

Lung, C.W. and Mu, Z.Q. (1987), "Fractal dimension measured with perimeter-area relation and toughness of materials", *Physics Review Bulletin*, **38**(16), 11781-11784.

Perdikaris, P.C. and Romeo, A. (1995), "Size effect on the fracture energy of concrete and stability issues in three point bending fracture toughness testing", *ACI Mater. J.,* **92**(5), 483-496.

Richardson, L.F. (1961), "The problem of contiguity: An appendix of statistics of deadly quarrels", *General System Yearbook*, **6**, 139-187.

Roh, Y.S. and Xi, Y. (2001), "The fracture surface roughness of concrete with different aggregate sizes and loading rates", ACI Special Publication, SP 201 - Fracture Mechanics for Concrete Materials: Testing and Applications, 35-54.

Saouma, V.E. and Barton, C.C. (1994), "Fractals, fractures and size effects in concrete", *J. Eng. Mech.,* ASCE, **120**(4), 835-854.

Trefilov, V.I., Kartuzov, V.V. and Minakov, N.V. (2001), "Fractal dimension of fracture surfaces", *Metal Science and Heat Treatment*, **43**(3-4), 95-98.

Wang, Y. and Diamond, S. (2001), "A fractal study of the fracture surface of cement pastes and mortars using a stereoscopic SEM method", *Cement and Concrete Research,* **31**, 1385-1392.

Xie, H. (1993), *Fractals in Rock Mechanics*, A.A. Balkema, Brookfield, Vt.

Zhang Z., Yu, J., Kou, S.Q. and Lindqvist, P-A. (2001), "On study of influences of loading rate on fractal dimensions of fracture surfaces in Gabbro", *Rock Mechanics and Rock Engineering*, **34**(3), 235-242.